The University of Osaka
Institutional Knowledge Archive

Title	Development of speckle-free channel-cut crystal optics using plasma chemical vaporization machining for coherent x-ray applications
Author(s)	Hirano, Takashi; Osaka, Taito; Sano, Yasuhisa et al.
Citation	Review of Scientific Instruments. 2016, 87(6), p. 063118
Version Type	VoR
URL	https://hdl.handle.net/11094/86949
rights	This article may be downloaded for personal use only. Any other use requires prior permission of the author and AIP Publishing. This article appeared in (citation of published article) and may be found at https://doi.org/10.1063/1.4954731.
Note	

The University of Osaka Institutional Knowledge Archive : OUKA

https://ir.library.osaka-u.ac.jp/

The University of Osaka

AIP | Review of Scientific Instruments

Development of speckle-free channel-cut crystal optics using plasma chemical vaporization machining for coherent x-ray applications

Takashi Hirano, Taito Osaka, Yasuhisa Sano, Yuichi Inubushi, Satoshi Matsuyama, Kensuke Tono, Tetsuya Ishikawa, Makina Yabashi, and Kazuto Yamauchi

Citation: Review of Scientific Instruments **87**, 063118 (2016); doi: 10.1063/1.4954731
View online: http://dx.doi.org/10.1063/1.4954731
View Table of Contents: http://scitation.aip.org/content/aip/journal/rsi/87/6?ver=pdfcov
Published by the AIP Publishing

Articles you may be interested in

Application of the rigorous method to x-ray and neutron beam scattering on rough surfaces
J. Appl. Phys. **108**, 033516 (2010); 10.1063/1.3467937

Coherent trapping of x-ray photons in crystal cavities in the picosecond regime
Appl. Phys. Lett. **93**, 141105 (2008); 10.1063/1.2996275

The Nanometer Optical Component Measuring Machine: a new Sub-nm Topography Measuring Device for X-ray Optics at BESSY
AIP Conf. Proc. **705**, 847 (2004); 10.1063/1.1757928

Application of optical scanner to switching of x-ray photon helicities at kHz range
Rev. Sci. Instrum. **74**, 19 (2003); 10.1063/1.1525877

Dynamical coherent illumination for X-ray microscopy at 3rd generation synchrotron radiation sources: First results with X-rays at the Ca-K edge (4 keV)
AIP Conf. Proc. **507**, 464 (2000); 10.1063/1.1291191

Reuse of AIP Publishing content is subject to the terms at: https://publishing.aip.org/authors/rights-and-permissions. Download to IP: 133.1.116.104 On: Thu, 21 Jul 2016 06:14:33

REVIEW OF SCIENTIFIC INSTRUMENTS **87**, 063118 (2016)

Development of speckle-free channel-cut crystal optics using plasma chemical vaporization machining for coherent x-ray applications

Takashi Hirano,[1,a)] Taito Osaka,[1] Yasuhisa Sano,[1] Yuichi Inubushi,[2] Satoshi Matsuyama,[1] Kensuke Tono,[2,3] Tetsuya Ishikawa,[3] Makina Yabashi,[3] and Kazuto Yamauchi[1]
[1]*Department of Precision Science and Technology, Graduate School of Engineering, Osaka University, 2-1 Yamada-oka, Suita, Osaka 565-0871, Japan*
[2]*Japan Synchrotron Radiation Research Institute (JASRI), 1-1-1, Kouto, Sayo-cho, Sayo-gun, Hyogo 679-5198, Japan*
[3]*RIKEN SPring-8 Center, 1-1-1 Kouto, Sayo-cho, Sayo-gun, Hyogo 679-5148, Japan*

(Received 6 April 2016; accepted 12 June 2016; published online 24 June 2016)

We have developed a method of fabricating speckle-free channel-cut crystal optics with plasma chemical vaporization machining, an etching method using atmospheric-pressure plasma, for coherent X-ray applications. We investigated the etching characteristics to silicon crystals and achieved a small surface roughness of less than 1 nm rms at a removal depth of >10 μm, which satisfies the requirements for eliminating subsurface damage while suppressing diffuse scattering from rough surfaces. We applied this method for fabricating channel-cut Si(220) crystals for a hard X-ray split-and-delay optical system and confirmed that the crystals provided speckle-free reflection profiles under coherent X-ray illumination. *Published by AIP Publishing.* [http://dx.doi.org/10.1063/1.4954731]

I. INTRODUCTION

The advent of third-generation synchrotron sources and X-ray free-electron lasers (XFELs) has opened new opportunities in various fields of science. Perfect crystal optical devices based on Bragg diffraction have been widely used to control beam conditions as monochromators, collimators, and phase retarders in the hard X-ray region.[1,2] The crystal optics, particularly with multiple crystal elements, are increasingly important for performing advanced applications with these advanced X-ray sources. For example, the combination of four crystals in highly asymmetric reflections provides an X-ray beam with an extremely narrow bandwidth for high-resolution X-ray spectroscopy.[3] Also, a split-and-delay optical (SDO) system[4] utilized for an XFEL source generates two X-ray pulses in a time interval controlled with sub-femtosecond accuracy, which enables the investigation of ultrafast atomic dynamics.

All optical devices should preserve the coherent wavefront without introducing any instability in order to fully utilize the unique capabilities of these advanced, low-emittance X-ray sources. However, it has been difficult to satisfy these requirements with multiple crystal optics. One can combine independent blocks of Si crystals with high-quality surface finish for preserving the coherent wavefront without speckles, whereas the use of a large number of independent crystals tends to yield instabilities in output beam properties, such as pointing and intensity, with increased complexity.

To improve stability with reduced complications in multiple crystal arrangements, the employment of a channel-cut crystal (CC),[5] which is a monolithic crystal with a groove separating two diffraction surfaces, is highly useful. Here, an X-ray beam is reflected twice at the two inner-wall surfaces with parallel lattice planes in the single crystal block. The direction of the exit beam from the CC is thus collinear to that of the incident beam with an extremely high accuracy that can potentially reach the nanoradian range.

However, it has been difficult to preserve the wavefront with CC devices owing to the difficulties in performing high-quality surface finishing of the inner walls using conventional techniques such as chemical mechanical polishing (CMP) or wet etching methods. The former method provides smooth and flat surfaces, although subsurface crystallographic damage that generates unwanted speckles in the reflected beam can be introduced for inner-wall processing. Note that some efforts toward improving the crystal perfection of CMP-finished surfaces have been reported.[6,7] The latter method can reduce subsurface damage, while inducing considerable surface roughness and undulation.[8–10] An undulated diffraction surface could distort the temporal structure of X-ray pulses, which becomes a serious problem for ultrafast X-ray sources, such as XFELs.

In this paper, we report a new method for fabricating high-quality CC optics with plasma chemical vaporization machining (PCVM), which is an etching method using atmospheric-pressure plasma.[11] PCVM is a purely chemical method that results in a crystallographically damage-free process. One can localize the plasma area to the specific processing area at ambient pressure. The utilization of localized plasma is useful for correcting figure errors by scanning the plasma with computer-controlled scan speeds. Also, the utilization of fluoride molecules as an etchant gas enables the isotropic removal of Si atoms with independence of crystal orientations owing to the high reactivity of the fluorine radical. By using this method, high-quality Si crystals with a thickness of ~10 μm and a surface roughness of ~0.1 nm rms, which can act as X-ray beam splitters, have been successfully fabricated.[12,13]

In this study, we applied PCVM to the fabrication of channel-cut Si(220) crystals utilized in an SDO system. We

a)Author to whom correspondence should be addressed. Electronic mail: hirano@up.prec.eng.osaka-u.ac.jp.

Reuse of AIP Publishing content is subject to the terms at: https://publishing.aip.org/authors/rights-and-permissions. Download to IP: 133.1.116.104 On: Thu, 21 Jul 2016 06:14:33

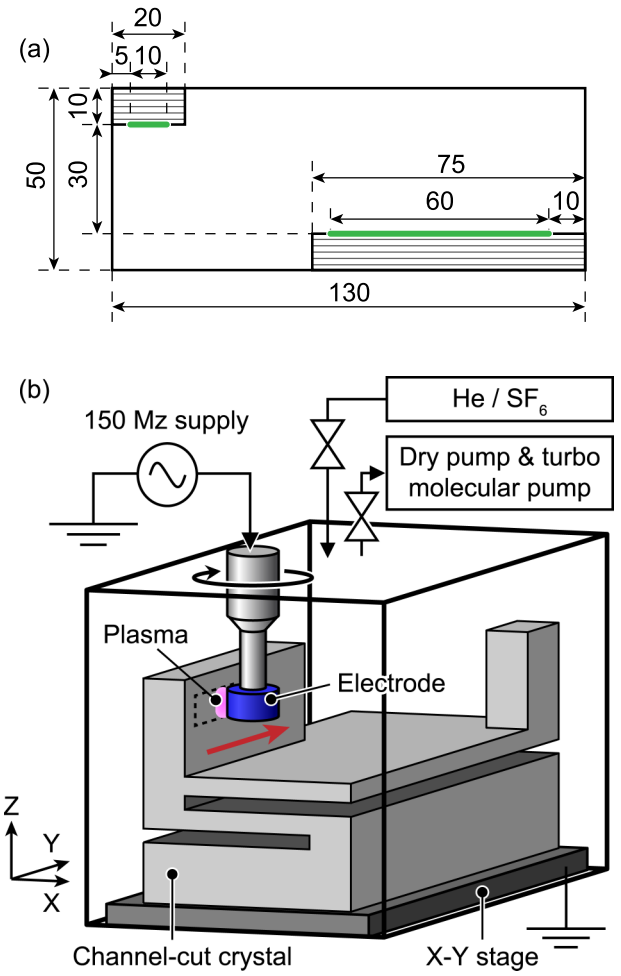

FIG. 1. (a) Dimensions of the channel-cut crystal (units: millimeters). The treated areas of inner-wall surfaces are highlighted by the green lines. (b) Schematic drawing of the equipment used in the inner-wall treatment. The electrode is inserted into the channel groove of the crystal and scanned along the Y-direction. The plasma was generated between the electrode and channel walls in a high-purity etchant environment (He and SF_6).

report on the details of the fabrication process and results of performance characterization of the crystals using coherent X-rays from SPring-8 and SPring-8 angstrom compact free-electron laser (SACLA).[14]

TABLE I. Typical removal conditions.

Pressure of ambient gas (kPa)	100
Ratio of He and SF_6	99.5:0.5
Gap between sample and electrode (mm)	0.2
Rotation speed of electrode (rpm)	5000
Electric power (W)	24

II. CRYSTAL FABRICATION

A. Crystal design and fabrication equipment

Figure 1(a) shows the dimensions of the CC employed in this study. Two CCs with symmetric shapes were prepared from a floating-zone (FZ) Si(220) single crystal ingot by cutting a groove with a width of 30 mm. The CC covers a photon-energy range of 6.5–11.5 keV. The as-received inner-wall surfaces were finished using conventional techniques with a roughness value of approximately 1 nm rms, involving scratches and defects. Empirically, the layers with a depth of at least 3 μm should be removed for the inner-wall surfaces in order to eliminate subsurface damage introduced with the fabrication processes before PCVM.[12] Note that more rough surfaces can be also smoothed to less than 1 nm rms via PCVM with more removal depth. Also, a removal width of >3 mm is necessary to ensure sufficient lateral spatial acceptance of the CC. The flatness of the diffraction surfaces is also important for maintaining the temporal structure of the incident X-ray pulses because path lengths of the reflection beams could be varied within the X-ray footprint. The geometric time delay Δt of the reflected beams can be written as

$$\Delta t = -\frac{2\Delta z \sin\theta_B}{c},$$

where Δz, θ_B, and c are the difference in height within the X-ray footprint, the Bragg angle, and the speed of light. A target value of the maximum surface undulation should be much smaller than 1.5 μm peak-to-valley (PV), corresponding to $\Delta t = 3.2$ fs at 10 keV, which is equivalent to the pulse duration determined from the Fourier limited condition of the Si(220) diffraction. The equipment used in the PCVM process is schematically depicted in Fig. 1(b). Ambient air in the chamber was evacuated to a pressure of 10^{-4} Pa and subsequently purged

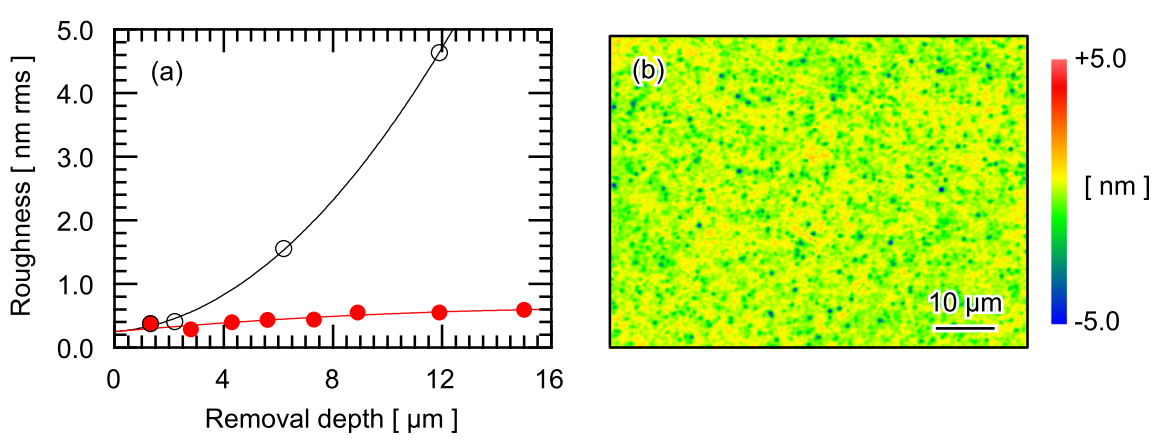

FIG. 2. (a) Averaged roughness for CZ-Si wafer as a function of removal depth with two scan methods. The results of the single-scan and multi-scan methods are shown as open black circles and closed red circles, respectively. (b) Measured surface morphology on the bottom of the removal profile with a depth of ~15 μm using the multi-scan method. The roughness is 0.535 nm rms in a 71×53 μm^2 area.

Reuse of AIP Publishing content is subject to the terms at: https://publishing.aip.org/authors/rights-and-permissions. Download to IP: 133.1.116.104 On: Thu, 21 Jul 2016 06:14:33

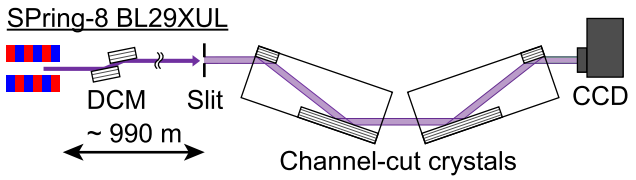

FIG. 3. Schematic diagram of experimental setup for X-ray topography measurements.

with a high-purity mixture of He and SF_6 gases. We used a cylinder-shaped electrode with a height and a diameter of 6 and 10 mm, respectively. A sample crystal was mounted on a grounded X-Y stage that allowed us to adjust the process area and the gap between the sample and the electrode. Rotating the electrode produced an one-directional laminar flow in the gap because of the high viscosity of the atmospheric-pressure gas. Accordingly, the etchant gas was precisely introduced into the plasma area while the reaction products (SiF_x) flowed out from the plasma area. Surface roughening caused by the re-deposition of the products can also be suppressed owing to the stable laminar flow.

B. Processing characteristics and fabrication results

The processing characteristics of PCVM were investigated using commercial Czochralski (CZ)-Si(001) wafers with roughness values of ~0.2 nm rms. Removal profiles and roughness values of the processed area were measured with a microscopic interferometer (Zygo, NewView 5032). Typical removal conditions are listed in Table I. A high proportion of He gas (99.5%) was required in order to stabilize the atmospheric-pressure plasma. The narrow gap and the high rotational speed of the electrode contributed to the generation of laminar flow with a high flow rate of ~1 m/s. A low electric power of ~30 W was applied in order to prevent an excess supply of energy from reaching the charged particles in the plasma. The scanning direction was the same as the direction of the gas flow in order to reduce the amount of re-deposition onto the finished surfaces.

Two approaches can be used to achieve sufficient removal depth: a single-scan method in which the scan speed of the electrode slowed down to 1–10 mm/min or a multi-scan method in which the scan speed was maintained at a relatively high value of 10 mm/min. Figure 2(a) shows a comparison of the surface roughness values associated with these methods. We found that the single-scan method provides significant surface roughness for increased removal depth, while the multi-scan method keeps a smooth surface roughness of <0.5 nm rms over a wide range of removal depths. The reason for the larger roughness in the single-scan method is considered to be the high amount of re-deposited contaminations on the surface around the plasma area. In the multi-scan method, the surface roughness introduced by one scan is small owing to the relatively high scan speed. Furthermore, the roughness decreased during the following scans. As a result, we were able to achieve a smoother surface, as shown in Fig. 2(b).

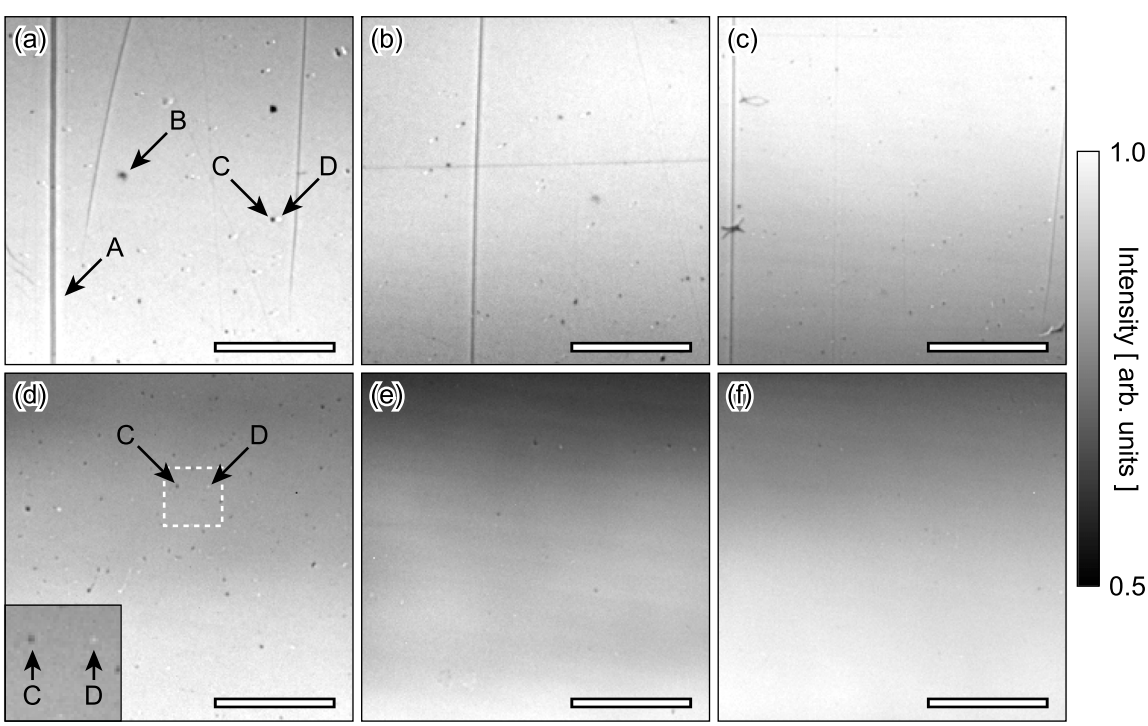

FIG. 4. Four-bounced Si(220) reflection topographs of channel-cut crystals arranged in a (+, −, −, +) geometry, measured ((a)–(c)) before and ((d)–(f)) after the inner-wall treatment. Topographs shown in left, center, and right columns were measured at photon energies of 7, 9, and 11 keV, respectively. The scale bars represent a length of 1 mm. The reflection images are normalized by the intensity profiles of the incident beams and displayed on optimized color scales with the same dynamic range. Low-frequency contrasts in all images were induced by intensity variations of the incident beams due to the vibrations of the double-crystal monochromator. Line-shaped (A) and dot-shaped (B) shadows correspond to subsurface damage. Dark and bright spots (see labels (C) and (D), for example), which originate from dust on the polyimide window of the beamline vacuum tube, were formed in pairs because of the positional translations of the reflected beams from that of incident beams in the horizontal direction due to imperfect angular adjustments of the crystals. Inset in panel (d) shows enlarged images of the pair as indicated by a dashed rectangle with a size of 1×1 mm^2 in panel (d).

Reuse of AIP Publishing content is subject to the terms at: https://publishing.aip.org/authors/rights-and-permissions. Download to IP: 133.1.116.104 On: Thu, 21 Jul 2016 06:14:33

All inner-wall surfaces of the two CCs were processed under optimized removal conditions. Since the FZ-Si crystals have a higher specific resistivity compared with that of the CZ-Si, we employed a lower gas pressure of 75 kPa and a higher electric power of ~40 W, as compared to the conditions shown in Table I. A trench-like removal profile with a width of ~4 mm was obtained, corresponding to the height of the electrode. The removal depth for each inner-wall surface was >3 μm, thus satisfying the requirements for eliminating the subsurface damage. The surface undulation was less than 200 nm PV within a typical XFEL footprint of 0.5 × 1.8 mm^2 at 11.5 keV in SACLA. The roughness of the finished inner-wall surfaces was less than 1 nm rms over the entire area.

III. EVALUATION WITH COHERENT X-RAYS

We measured X-ray reflection profiles with a pair of CCs operated in a (+, −, −, +) arrangement (a setup used in the SDO system) at the 1 km long beamline BL29XUL of SPring-8.[15] The experimental setup is schematically shown in Fig. 3. An X-ray beam from the Si(111) double-crystal monochromator was transported to the first crystal located 1 km downstream from the source. The long beam transport enhanced the transverse coherent area over the sample area and suppressed beam divergence to the level of several microradians. Four-bounced reflection profiles were captured with a CCD camera (Hamamatsu, ORCA-RII, effective pixel size: 13 μm) at various photon energies within the range of 6.5–12.0 keV.

Figure 4 shows the four-bounced Si(220) reflection topographs around peak reflectivities, taken before and after the PCVM process, with photon energies of 7, 9, and 11 keV. A number of spots and scratches originating from the subsurface damage were observed in the whole photon energy range before the PCVM process, as shown in Figs. 4(a)–4(c). After the process, we obtained almost uniform intensity distributions in the processed area [Figs. 4(d)–4(f)]. Note that pairs of dark and bright spots (see labels C and D in Figs. 4(a) and 4(d), for example) are caused by dust on the polyimide window of the beamline vacuum tube, and that most of the spots in Fig. 4(d) are assigned as these pairs. This result indicates that the subsurface damage was successfully removed via PCVM.

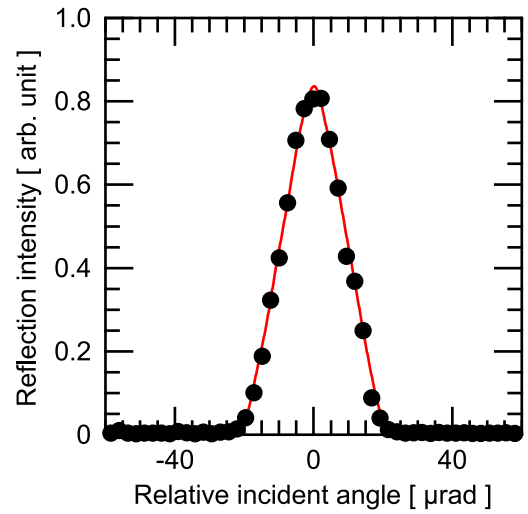

FIG. 6. Rocking curve measure with rotation of the second channel-cut Si(220) crystal at 10 keV. The crystals were arranged in the similar setup as shown in Fig. 3. The divergence of the incidence was ~2 μrad in full-width at half maximum. Experimental points and calculated curves are shown as closed black circles and red solid lines, respectively.

We also tested the performance of the crystals at BL3 of SACLA, operated with a repetition rate of 30 Hz at 10 keV. The XFEL pulses provided excellent transverse coherence and a divergence of ~2 μrad in full-width at half maximum (FWHM). Figure 5(a) shows an averaged profile of the incident XFEL beam without the CCs taken with a complementary metal oxide semiconductor (CMOS) camera (Hamamatsu, ORCA-Flash4.0, effective pixel size: 1.2 μm), placed at ~100 m and ~1 m downstream from the undulator exit and the second CC, respectively. The averaged beam profile reflected on un-treated areas of the CCs displays some shadow lines and dots owing to the residual damage [Fig. 5(b)]. In contrast, at the treated parts, we obtained a good reflection profile without damage-induced speckles, as shown in Fig. 5(c), which is similar to that of the incident beam. At some treated parts, weak speckles were observed in the reflection profiles, which were considered to originate from small residual defects. Although the removal depth of 3 μm may be insufficient for eliminating damage, further removal up to ~10 μm without surface roughening can be achieved by means of the multi-scan method. Figure 6 shows a rocking curve measured with

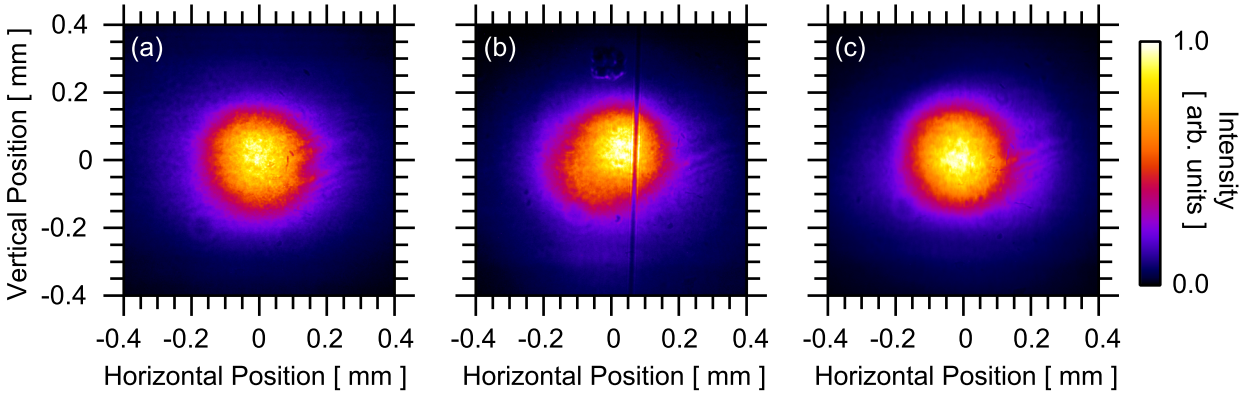

FIG. 5. Averaged beam profiles measured at SACLA. (a) Direct beam without channel-cut crystals. Monochromatic beams from channel-cut crystals with (b) un-treated and (c) treated parts.

Reuse of AIP Publishing content is subject to the terms at: https://publishing.aip.org/authors/rights-and-permissions. Download to IP: 133.1.116.104 On: Thu, 21 Jul 2016 06:14:33

rotation of the second CC. The experimental result agreed with the theoretical curves calculated using the dynamical theory of diffraction, indicating excellent diffraction qualities of the treated inner-wall surfaces.

IV. CONCLUSION AND PERSPECTIVE

We have developed a new fabrication method using the PCVM technique in order to produce speckle-free channel-cut Si(220) crystals for utilization in the SDO system. We achieved a successful removal of the subsurface damage while maintaining high smoothness by means of the one-axis multi-scan method, which resulted in the preservation of the X-ray wavefront at SPring-8 and SACLA. This result confirms the feasibility of using CCs in coherent applications that require speckle-free X-ray beams with extremely stable beam conditions. More precise measurements will be performed to evaluate the reduction of the diffused scattering via PCVM from low-reflectivity tails of the rocking curves.

The PCVM technique can be applied to various types of monolithic crystal optics,[16–19] such as inner-walls of narrow-channel crystals with a channel width smaller than a few millimeters, by using a dedicated electrode; this expands the range of applications that utilize CCs for quick scanning X-ray absorption fine structure studies,[20,21] multi-bounce monochromators for decreasing spectral tails,[5] and compact monochromators for self-seeded XFELs with reasonable chicane lengths below 10 m. PCVM can also address the deterministic processing (e.g., high-precision surface flattening and thinning) of inner-wall surfaces by means of the two-dimensional scanning of highly localized plasma. As one of the interesting applications of this technique, a multi-blade crystal monochromator (a so-called "comb crystal")[22] for micro-electronvolt energy resolution could be realized by imposing strict requirements on the thickness, flatness, roughness, and spacing. This study represents an important step towards the development of these complex optical devices.

ACKNOWLEDGMENTS

The synchrotron radiation experiments were performed at BL29XUL in SPring-8 with the approval of RIKEN (Proposal Nos. 20130033, 20140013, and 20150075). The use of the beamline BL3 at SACLA was supported by RIKEN. The authors wish to thank the staff of SPring-8/SACLA for their support and valuable discussions. This study was partially supported by X-ray Free Electron Laser Priority Strategy Program (MEXT) and Program for Leading Graduate Schools: "Interactive Materials Science Cadet Program."

[1]M. Hart, Rep. Prog. Phys. **34**, 435 (1971).
[2]M. Yabashi, K. Tamasaku, K. Sawada, S. Goto, and T. Ishikawa, "Perfect crystal optics," in *Synchrotron Light Sources Free-Electron Lasers*, edited by E. Jaeschke, S. Khan, J. R. Schneider, and J. B. Hastings (Springer International Publishing, Cham, 2016).
[3]M. Yabashi, K. Tamasaku, S. Kikuta, and T. Ishikawa, Rev. Sci. Instrum. **72**, 4080 (2001).
[4]T. Osaka, T. Hirano, Y. Sano, Y. Inubushi, S. Matsuyama, K. Tono, T. Ishikawa, K. Yamauchi, and M. Yabashi, Opt. Express **24**, 9187 (2016).
[5]U. Bonse and M. Hart, Appl. Phys. Lett. **7**, 238 (1965).
[6]A. V. Zozulya, A. Shabalin, H. Schulte-Schrepping, J. Heuer, M. Spiwek, I. Sergeev, I. Besedin, I. A. Vartanyants, and M. Sprung, J. Phys.: Conf. Ser. **499**, 012003 (2014).
[7]E. Kasman, M. Erdmann, and S. Stoupin, Proc. SPIE **9590**, 95900D (2015).
[8]A. Gabrielli, A. Baldassarri, and B. Sapoval, Phys. Rev. E **62**, 3103 (2000).
[9]P. K. Dhillon and S. Sarkar, Appl. Surf. Sci. **284**, 569 (2013).
[10]M. Shikida, T. Masuda, D. Uchikawa, and K. Sato, Sens. Actuators, A **90**, 223 (2001).
[11]Y. Mori, K. Yamauchi, K. Yamamura, and Y. Sano, Rev. Sci. Instrum. **71**, 4627 (2000).
[12]T. Osaka, M. Yabashi, Y. Sano, K. Tono, Y. Inubushi, T. Sato, S. Matsuyama, T. Ishikawa, and K. Yamauchi, Key Eng. Mater. **523-524**, 40 (2012).
[13]T. Osaka, M. Yabashi, Y. Sano, K. Tono, Y. Inubushi, T. Sato, S. Matsuyama, T. Ishikawa, and K. Yamauchi, Opt. Express **21**, 2823 (2013).
[14]T. Ishikawa, H. Aoyagi, T. Asaka, Y. Asano, N. Azumi, T. Bizen, H. Ego, K. Fukami, T. Fukui, Y. Furukawa, S. Goto, H. Hanaki, T. Hara, T. Hasegawa, T. Hatsui, A. Higashiya, T. Hirono, N. Hosoda, M. Ishii, T. Inagaki, Y. Inubushi, T. Itoga, Y. Joti, M. Kago, T. Kameshima, H. Kimura, Y. Kirihara, A. Kiyomichi, T. Kobayashi, C. Kondo, T. Kudo, H. Maesaka, X. M. Maréchal, T. Masuda, S. Matsubara, T. Matsumoto, T. Matsushita, S. Matsui, M. Nagasono, N. Nariyama, H. Ohashi, T. Ohata, T. Ohshima, S. Ono, Y. Otake, C. Saji, T. Sakurai, T. Sato, K. Sawada, T. Seike, K. Shirasawa, T. Sugimoto, S. Suzuki, S. Takahashi, H. Takebe, K. Takeshita, K. Tamasaku, K. Tono, S. Wu, M. Yabashi, M. Yamaga, A. Yamashita, K. Yanagida, C. Zhang, T. Shintake, H. Kitamura, and N. Kumagai, Nat. Photonics **6**, 540 (2012).
[15]K. Tamasaku, Y. Tanaka, M. Yabashi, H. Yamazaki, N. Kawamura, M. Suzuki, and T. Ishikawa, Nucl. Instrum. Methods Phys. Res., Sect. A **467-468**, 686 (2001).
[16]J. Hrdý, P. Mikulík, and P. Oberta, J. Synchrotron Radiat. **18**, 299 (2011).
[17]D. Korytár, P. Vagovic, K. Végsö, P. Siffalovic, E. Dobrocka, W. Jark, V. Ác, Z. Záprazný, C. Ferrari, A. Cecilia, E. Hamann, P. Mikulík, T. Baumbach, M. Fiederle, and M. Jergel, J. Appl. Crystallogr. **46**, 945 (2013).
[18]J. P. Sutter, T. Ishikawa, U. Kuetgens, G. Materlik, Y. Nishino, A. Rostomyan, K. Tamasaku, and M. Yabashi, J. Synchrotron Radiat. **11**, 378 (2004).
[19]T. Inada, T. Yamaji, S. Adachi, T. Namba, S. Asai, T. Kobayashi, K. Tamasaku, Y. Tanaka, Y. Inubushi, K. Sawada, M. Yabashi, and T. Ishikawa, Phys. Lett. B **732**, 356 (2014).
[20]R. Frahm, Rev. Sci. Instrum. **60**, 2515 (1989).
[21]O. Müller, D. Lützenkirchen-Hecht, and R. Frahm, Rev. Sci. Instrum. **86**, 093905 (2015).
[22]See https://www.bnl.gov/nsls2/docs/PDF/cdr/4_IXS%20CDRfinal_10_10%20BAT.pdf for Conceptual design report for the inelastic x-ray scattering beamline at NSLS-II (LT-XFD_CDR_IXS-00123), final draft 2 October 2009, section 2.4: Optical Layout.

Reuse of AIP Publishing content is subject to the terms at: https://publishing.aip.org/authors/rights-and-permissions. Download to IP: 133.1.116.104 On: Thu, 21 Jul 2016 06:14:33